

УДК: 532.5.032, 532.517.3

Численное моделирование течения Колмогорова в вязких средах под действием периодической в пространстве статической силы

В. В. Денисенко¹, А. Н. Долуденко², С. В. Фортова^{1,а}, И. В. Колоколов³,
В. В. Лебедев³

¹Институт автоматизации проектирования РАН,
Россия, 123056, Москва, ул. 2-я Брестская, д. 19/18

²Институт высоких температур РАН,

Россия, 125412, г. Москва, ул. Ижорская, д. 13, стр. 2

³Институт теоретической физики им. Л. Д. Ландау РАН,
Россия, 142432, Московская обл., г. Черноголовка, просп. Академика Семенова, д. 1а

E-mail: ^а sfortova@mail.ru

Получено 13.12.2021.

Принято к публикации 01.03.2022.

Основной особенностью двумерного турбулентного течения, постоянно возбуждаемого внешней силой, является возникновение обратного каскада энергии. За счет нелинейных эффектов пространственный масштаб вихрей, создаваемых внешней силой, увеличивается до тех пор, пока рост не будет остановлен размером ячейки. В последнем случае энергия накапливается на этом масштабе. При определенных условиях такое накопление энергии приводит к возникновению системы когерентных вихрей. Наблюдаемые вихри имеют размер ячейки и в среднем изотропны. Численное моделирование является эффективным способом изучения таких процессов. Особый интерес представляет задача исследования турбулентности вязкой жидкости в квадратной ячейке при возбуждении коротковолновой и длинноволновой статическими внешними силами. Численное моделирование проводилось со слабосжимаемой жидкостью в двумерной квадратной ячейке с нулевыми граничными условиями. В работе показано, как на характеристики течения влияет пространственная частота внешней силы, а также величина вязкости самой жидкости. Увеличение пространственной частоты внешней силы приводит к стабилизации и ламинаризации течения. В то же время при увеличении пространственной частоты внешней силы уменьшение вязкости приводит к возобновлению механизма переноса энергии по обратному каскаду за счет смещения области диссипации энергии в область меньших масштабов по сравнению с масштабом накачки.

Ключевые слова: течение Колмогорова, вихрь, турбулентность

Работа выполнена при поддержке Министерства науки и высшего образования Российской Федерации (госзадания № 075-01056-22-00, № АААА-А19-119041590048-0 и 075-15-2019-1893).

UDC: 532.5.032, 532.517.3

Numerical modeling of the Kolmogorov flow in a viscous media, forced by the static force periodic in space

V. V. Denisenko¹, A. N. Doludenko², S. V. Fortova^{1,a}, I. V. Kolokolov³,
V. V. Lebedev³

¹Institute for Computer Aided Design of the RAS,
19/18 2-nd Brestskaya st., Moscow, 123056, Russian Federation

²Joint Institute for High Temperatures of the RAS,
13/2 Izhorskaya st., Moscow 125412, Russia

³Landau Institute for Theoretical Physics of the RAS,
1A Akademika Semenova av., Chernogolovka, Moscow region, 142432, Russia

E-mail: ^a sfortova@mail.ru

Received 13.12.2021.

Accepted for publication 01.03.2022.

The main feature of a two-dimensional turbulent flow, constantly excited by an external force, is the appearance of an inverse energy cascade. Due to nonlinear effects, the spatial scale of the vortices created by the external force increases until the growth is stopped by the size of the cell. In the latter case, energy is accumulated at these dimensions. Under certain conditions, accumulation leads to the appearance of a system of coherent vortices. The observed vortices are of the order of the box size and, on average, are isotropic. Numerical simulation is an effective way to study such the processes. Of particular interest is the problem of studying the viscous fluid turbulence in a square cell under excitation by short-wave and long-wave static external forces. Numerical modeling was carried out with a weakly compressible fluid in a two-dimensional square cell with zero boundary conditions. The work shows how the flow characteristics are influenced by the spatial frequency of the external force and the magnitude of the viscosity of the fluid itself. An increase in the spatial frequency of the external force leads to stabilization and laminarization of the flow. At the same time, with an increased spatial frequency of the external force, a decrease in viscosity leads to the resumption of the mechanism of energy transfer along the inverse cascade due to a shift in the energy dissipation region to a region of smaller scales compared to the pump scale.

Keywords: Kolmogorov flow, vortex, turbulence

Citation: *Computer Research and Modeling*, 2022, vol. 14, no. 4, pp. 741–753.

This work was supported by the Ministry of Science and Higher Education of the Russian Federation (State Assignments No. 075-01056-22-00, No. AAAA-A19-119041590048-0 и No. 075-15-2019-1893).

1. Introduction

Turbulence in liquid and gas is the most common type of flow in the nature. Such a flow is, of course, a three-dimensional phenomenon. However, for example, in the Earth's atmosphere, such three-dimensional flows can be considered as quasi-two-dimensional flows. This can be done quite rightly because of the small height of the troposphere compared to both the dimensions of the formed vortex structures and the distances over which they move.

It was found that the nature of the two-dimensional turbulent flows differs significantly from the three-dimensional turbulence [Kraichnan, 1967; Batchelor, 1969]. In the latter the energy is transferred from the larger vortices to the smaller ones, while in the two-dimensional turbulence, on the contrary, the transfer cascade leads to an enlargement of vortex structures. A typical example is the formation of cyclones, anticyclones, hurricanes in the Earth's atmosphere.

It would be more natural to consider the two-dimensional turbulence in an unlimited space. Of course, during modeling it is impossible to provide exactly such conditions, but one can imagine the unlimited space with the periodic boundary conditions. This kind of modeling was carried out in [Chertkov et al., 2007; Laurie et al., 2014]. With this approach, a dipole consisting of two vortices rotating in the opposite directions is ultimately formed.

When setting up a real experiment, it is also impossible to provide the periodic boundary conditions. Usually, the experiment is conducted in a closed volume — an experimental cell, which is bounded by walls [Sommeria, 1986]. In order to bring the calculations closer to the experiment during modeling, it is necessary to set zero boundary conditions (with adhesion to the walls), since in the experiment a viscous fluid acts as the medium under consideration.

To observe the reverse cascade in an experiment, it is necessary to act on a viscous fluid with an external periodic force. Usually the spatial frequency is such that the width of the experimental cell is equal to several wavelengths of the external force. In the general case, the nature of this external force, changing over time, determines the energy input into the system and, accordingly, the parameters of vortex formation in liquid. However, in many experiments [Gledzer et al., 2011; Xia, Shats, Falkovich, 2009] the external exciting force, intended for studying the appearance of coherent structures in the two-dimensional system, is constant over time. In [Kolokolov, Lebedev, 2017], the characteristics of large-scale turbulent motion are analyzed through the parameters of static, i. e., time-invariant exciting force.

In experimental studies, in general, just one conductive fluid is used. Even if the fluid is another one, neither the considered density nor the viscosity will change dramatically. In addition, in the experiment it is possible to adjust the amplitude of the external force and its spatial frequency, but also in a rather narrow range. The aim our work is, firstly, to obtain results that correspond to those obtained in the experiment. They validate our numerical algorithm. And, secondly, to carry out calculations with parameters that are obviously beyond the scope of the experiment. This is necessary to understand, for example, under what parameters a transition from laminar to turbulent flow can occur. Actually, this is the novelty of the study: consideration of a pseudo-two-dimensional flow, taking into account different combinations of the external force amplitude, its spatial frequency and fluid viscosity. All these have a rather significant effect on the nature of the resulting of two-dimensional flow.

2. Description of the experiment

The numerical simulation presented in this paper is an interpretation of the experiment, which can be found in [Gledzer, Dolzhanskij, Obuxov, 1981]. The experimental design is shown in Figure 1.

In this experiment, a planar horizontal rectangular cell was filled with the aqueous solution of electrically conductive electrolyte (CuSO_4). Using electrodes mounted on the longitudinal side walls

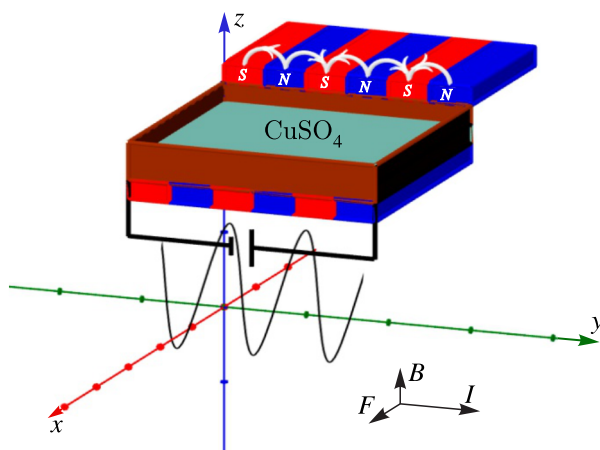


Figure 1. Schematic diagram of the experiment

of the cell, direct current was passed through electrolyte in the longitudinal direction. This cell with electrolyte was fixed on a sheet of magnetoelastic rubber, which served as a source of the external magnetic field (see Figure 1). Sources of the magnetic field were located so the magnetic field was created with a profile close to sinusoidal. Thus, the Lorentz electromagnetic force acted on the moving fluid in the transverse direction.

The present work has to simulate this kind of experiment with the parameters closest to those used. To do this, simulation results are presented for problems starting with simple ones, gradually complicating them with changes in the characteristics of both the external force and the properties of liquid itself.

3. Statement of the problem

Consider the problem of the plane flow of a viscous weakly compressible fluid under the action of an external periodic force directed along the Ox axis, periodical along the Oy axis and equal to $\rho G \sin(ky)$. Here $G = 0,01$ (N/kg) is the Lorentz force caused by the motion of electrically conductive fluid under the influence of an electric field and the action of an external magnetic field. The magnetic induction vector is perpendicular to the fluid motion. k is the wave number that determines the period of that magnetic force in space. The magnitude of the force G was obtained in experiments with conductive fluid, conducted by other researchers. This force remains constant over time.

The motion of the liquid medium in this case is described by the Navier–Stokes equations:

$$\begin{aligned} \frac{\partial \rho}{\partial t} + \nabla \cdot (\rho \mathbf{V}) &= 0, \\ \frac{\partial \rho u}{\partial t} + \nabla \cdot (\rho u \mathbf{V}) &= -\frac{\partial p}{\partial x} + \rho G \sin ky + \mu \Delta u, \\ \frac{\partial \rho v}{\partial t} + \nabla \cdot (\rho v \mathbf{V}) &= -\frac{\partial p}{\partial y} + \mu \Delta v, \\ \frac{dp}{d\rho} &= \frac{1}{\rho\beta}. \end{aligned} \quad (1)$$

Here $\mathbf{V} = (u, v)^T$ is the vector whose components are equal to the projections of velocity on the coordinate axis Ox and Oy , respectively; p is the pressure; ρ is the fluid density, and β is the artificial compressibility factor.

The fluid flow is considered in a square area of 128×128 computational cells. The length of the side of this area is $L = 2\pi$. The boundary conditions are the conditions of adhesion to the walls:

$$\mathbf{V}|_{\partial\Omega} = 0,$$

where $\partial\Omega$ is the entire boundary of the computational domain Ω .

The initial conditions are:

$$\begin{aligned} P(t = 0) &= P_0 = 10^5 \text{ Pa}, \\ \rho &= 1000 \text{ kg/m}^3, \\ \mu &= 2 \text{ Pa} \cdot \text{s}, \\ u(t = 0) &= 0,1 \sin(k_V y), \end{aligned} \tag{2}$$

$$v(t = 0) = -0,1 \sin(k_V x). \tag{3}$$

Conditions (2) and (3) on the initial perturbation of the velocity field satisfy the condition of field divergence $\text{div}(\mathbf{V}) = 0$. As further calculations showed, the initial field practically does not affect the nature of the steady flow. The latter is determined by the amplitude of the external force and its frequency.

4. Numerical method

The numerical calculation method used to simulate a viscous liquid medium is based on the explicit MacCormack method, which has a second order of accuracy in time and space. This method has proven itself in solving the hyperbolic equations of gas and hydrodynamics. In this problem, the Navier–Stokes equations are solved by the method of artificial compressibility [Anderson, Tannehill, Pletcher, 1984]. In this case, the hyperbolic part of the equations is solved by the MacCormack method, and the parabolic part is solved by the standard finite difference method. In this instance, there are no difficulties arising in solving the equations of an incompressible medium. Moreover, the degree of compressibility is a variable quantity that directly affects the propagation velocity of disturbances. This speed should be greater than the possible maximum flow velocities that arise during the simulation.

Every calculation stage on each time step in the MacCormack scheme is divided into 4 steps: forward differences and backward finite differences at the predictor stage along the Ox direction, and forward differences and backward differences at the predictor stage along the Oy direction. At the corrector stage, it is similar, except that the step «forward» changes to «backward» one. These steps cyclically change each other with each time step. Thus, the spatial symmetry of the solution along both axes Ox and Oy is observed.

We have used a rather coarse mesh with the size of 128×128 cells. Of course, such a coarse grid is not enough to model turbulent flows — in this case, resolutions on a small scale are usually implied. We are, on the contrary, interested in the large scales. But in this case pictures of the flow as a whole and the main integral characteristics will be approximately the same. For example, in Figure 2 one can see how the kinetic energy and enstrophy are changed with time using different meshes with the conditions under consideration. Here one can see the moment (time equals 5 s.) of destruction of the laminar flow and its transition to chaotic. So, calculations with the mesh used gives results corresponding to the finer grids.

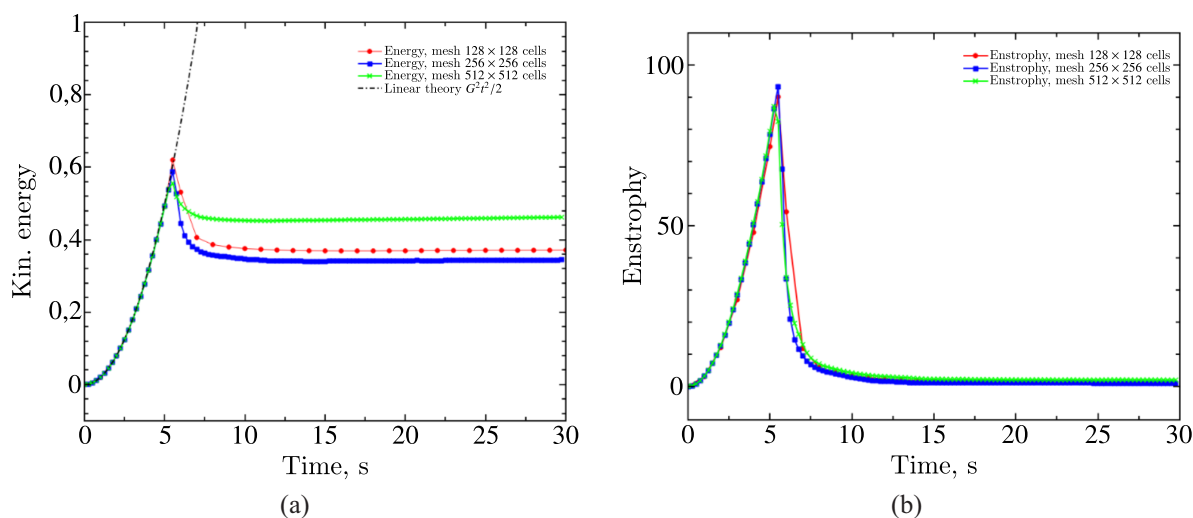


Figure 2. Integral kinetic energy a) and enstrophy b), using different mesh grids

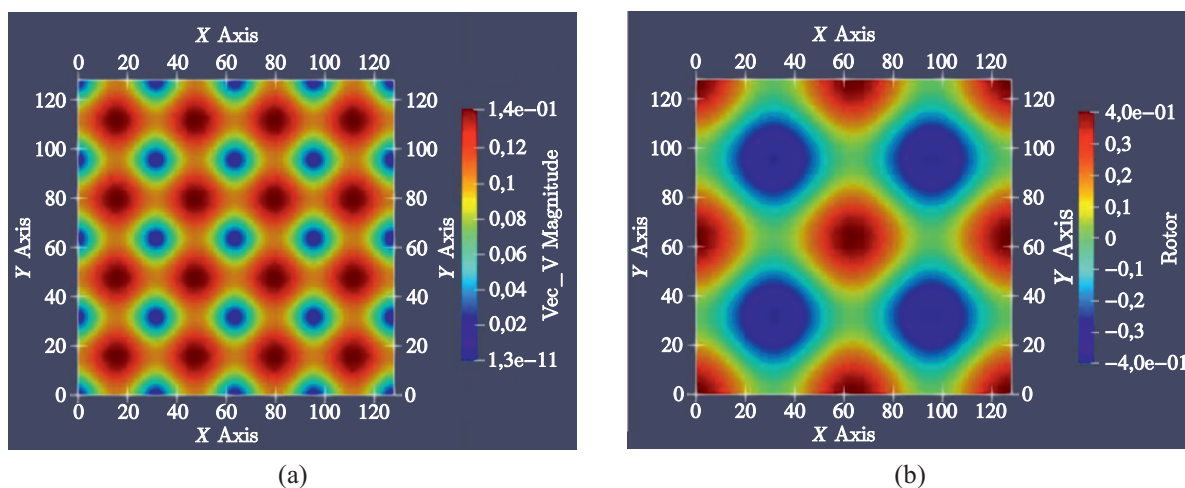


Figure 3. The initial distribution of velocity (a) and vorticity (b) for the problem with initial conditions defined by equations (2) and (3) for $k_v = 2$

5. Results

In the simplest formulation of the problem, the external force $G \sin(ky)$ along the Ox axis is equal to $0,01 \sin(2y)$. The perturbation of the initial velocity field corresponds to equations (2) and (3). The amplitude values of the initial velocity field are shown in Figure 3, *a*. The initial vorticity distribution is shown in Figure 3, *b*.

As a result of the flow development, a quasi-stationary flow arises, which is a single vortex. The center of this vortex oscillates around the center of the cell with a period of $T_V \approx 38$ s. The distance from the center of the vortex to the center of the cell is 18 calculated cells or 0,88 m (see Figure 4). In this case, the vortex itself rotates about to its center with a period of 35,6 s. Thus, the rotation period of the vortex itself almost coincides with the period of rotation of the vortex around the center of the cell under consideration.

The dependence of the tangential velocity of the vortex on the radius is shown in Figure 5. Here one can see the velocity profile in the numerically created vortex (blue triangles and red circles) and theoretical prediction, marked as black solid line.

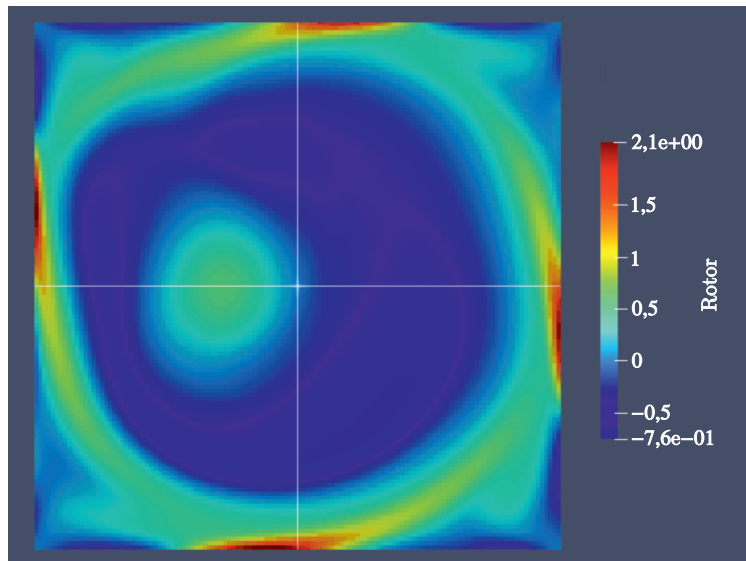


Figure 4. Vorticity distribution during quasistationary motion with the external force along the axis Ox equals $0,01 \sin(2y)$ at $k_V = 2$ under the initial conditions (2) and (3). The intersection of white lines indicates the center of the cell

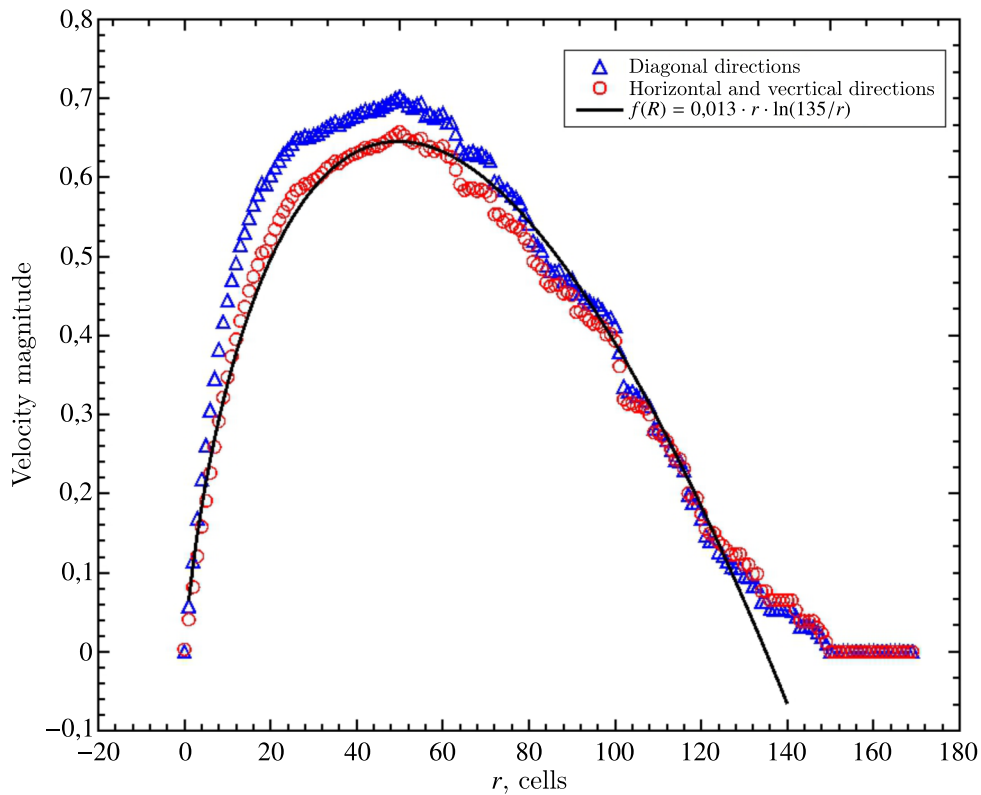


Figure 5. Dependence of the total and tangential velocities of the elementary volume fluid in the vortex on the radius, averaged over four mutually perpendicular directions

The Reynolds number is calculated as

$$Re = \frac{\rho V_{\max} L}{\mu}, \tag{4}$$

where $V_{\max} \approx 0,5$ m/s is the maximum fluid flow rate at the end of the calculation. The Reynolds number will be $Re \approx 1570$. In this variant of calculation, the artificial compressibility is taken to be

$$\frac{d\rho}{dp} = \rho\beta = 0,5 \left(\frac{\text{kg}}{\text{Pa} \cdot \text{m}^3} \right) \text{ or } 0,5 \left(\frac{\text{s}^2}{\text{m}^2} \right),$$

which provides the local sound speed equal to

$$c = \sqrt{\frac{dp}{d\rho}}, \quad c \approx 1,4 \frac{\text{m}}{\text{s}}.$$

In this case, the kinetic energy and the enstrophy, normalized to their maximum values, oscillate with the same period $T_{\text{En}} = 64$ s at steady flow (Figure 6). The ratio of the kinetic energy oscillation period and the rotation period of the vortex around the center of the cell equals $\frac{T_{\text{En}}}{T_V} \approx 1,68$.

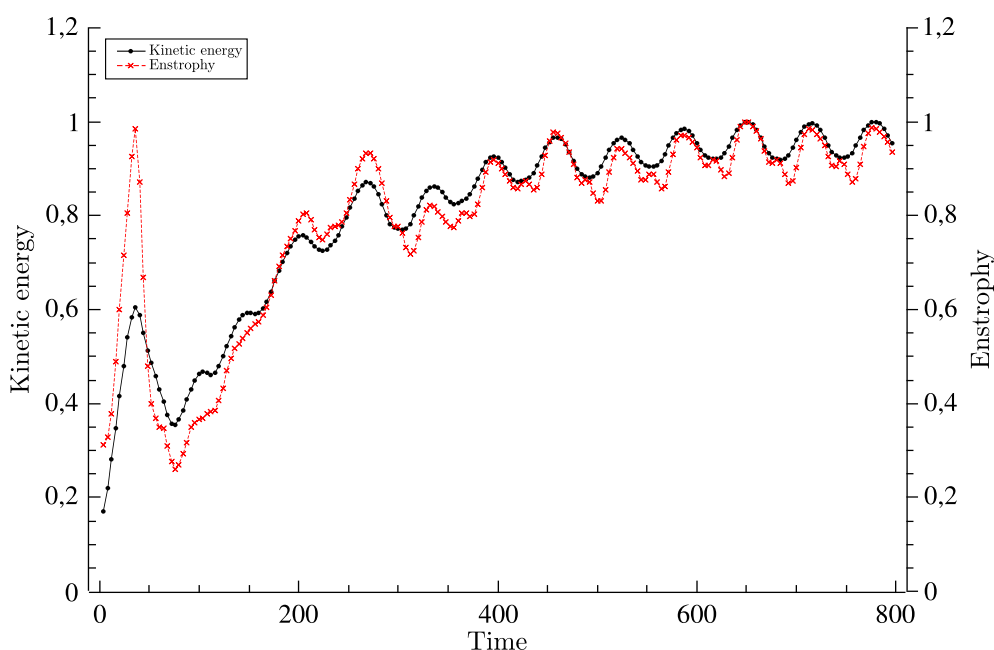


Figure 6. The kinetic energy and the enstrophy graphs normalized to their maximum values during quasi-stationary motion with the external force along the Ox axis equals $0,01 \sin(2y)$ and $k_V = 2$ under the initial conditions (2) and (3)

If the wave number $k_V = 2$ is increased under the initial conditions (2) and (3) to, for example, $k_V = 20$, then the steady-state form of the flow will be similar to that which occurs when $k_V = 2$ and the remaining parameters are unchanged. The same thing happens with any other wave number. Thus, steady motion is determined by the external force, and not by the initial velocity distribution.

With an increase in the amplitude of the external force (which can be associated, for example, with an increase in the magnetic field induction), the period of the vortex rotation around the cell center decreases, and the distance from its center to the cell center slightly increases.

For example, when the amplitude of the external force increases to $G = 0,02$ N/kg and the remaining parameters are fixed, according to the initial conditions given above, the period of revolution of the vortex around the center of the cell is $T_V \approx 24$ s, the distance of its center from the cell center is 22 numerical cells or $\approx 1,08$ m. The Reynolds number at steady state flow determined according to equation (4) is $Re \approx 2638$. The frequency of fluctuations of the kinetic energy and the enstrophy values increases (see Figure 7), and their period $T_{\text{En}} = 11,6$ s. The ratio of periods is $\frac{T_{\text{En}}}{T_V} \approx 0,48$.

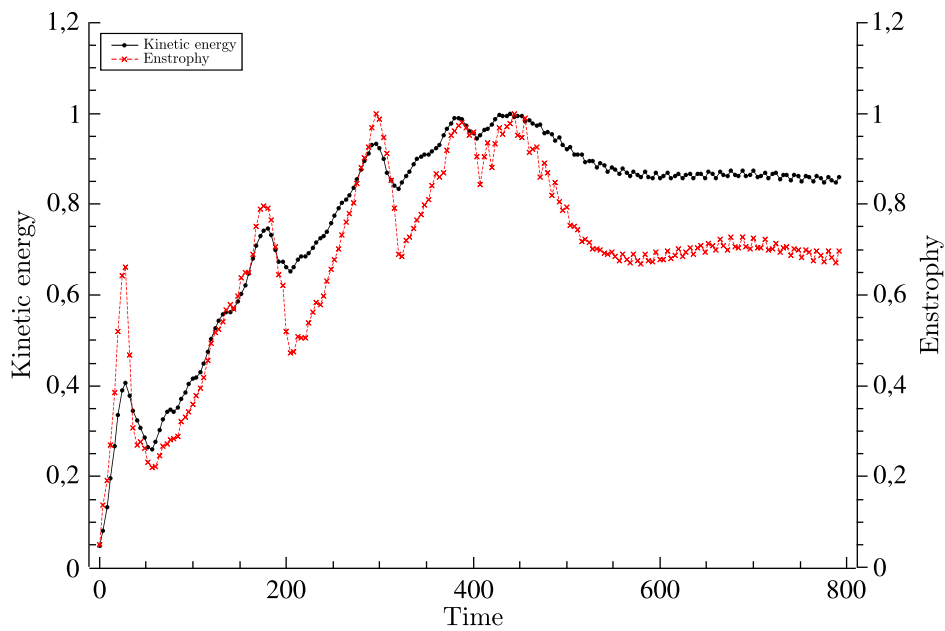


Figure 7. The kinetic energy and the enstrophy graphs normalized to their maximum values during quasi-stationary motion with the external force along the Ox axis equals $0,02 \sin(2y)$ and $k_V = 2$ under the initial conditions (2) and (3)

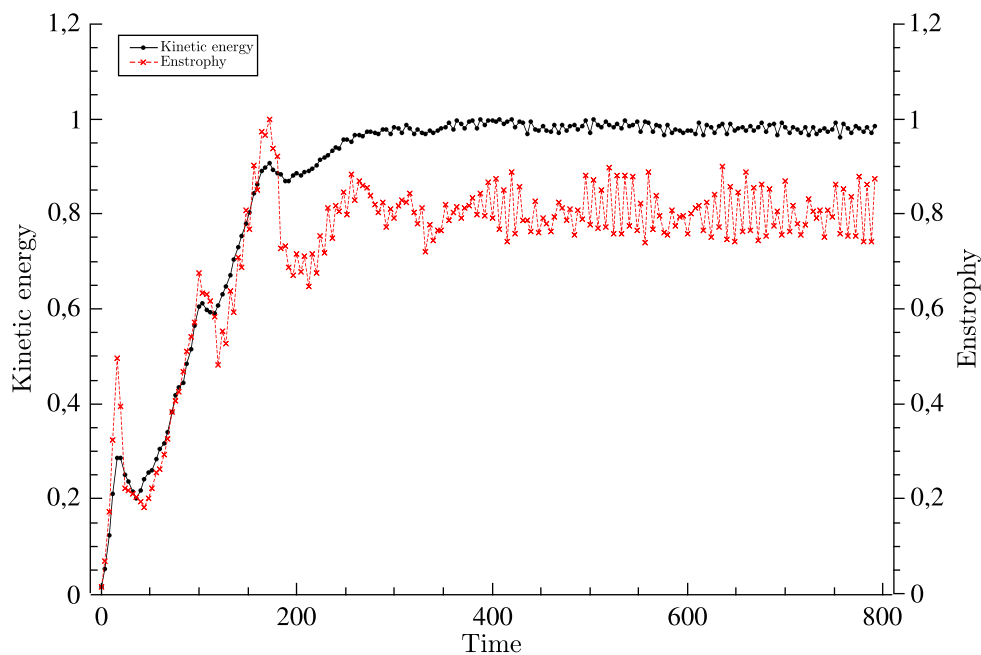


Figure 8. The kinetic energy and the enstrophy graphs normalized to their maximum values during quasi-stationary motion with the external force along the Ox axis equals $0,05 \sin(2y)$ and $k_V = 2$ under the initial conditions (2) and (3)

With an increase in the amplitude of the external force to $G = 0,05$ N/kg, the rotation period of the vortex around the cell center will be equal to $T_V \approx 12$ s. The distance of its center from the cell center will be 21 numerical cells or $\approx 1,03$ m. In this case, the frequency of fluctuations of both the kinetic energy and the enstrophy will increase slightly and their period will be $T_{En} \approx 10,4$ s. The ratio

will be $\frac{T_{En}}{T_V} \approx 1,5$ for the enstrophy and $\approx 1,15$ for the kinetic energy. The graph of changes in these quantities over time can be seen in Figure 8. The Reynolds number at steady state is $Re \approx 5340$.

If we increase the spatial frequency of the external force and put in the equation of motion along the Ox axis $k = 20$, and leave the value $k_V = 2$ in the equations describing the initial velocity distribution, then no vortex is formed over time, but a laminar flow is observed from the beginning to the very end of the calculation (Figure 9). On the pumping scale, when 20 characteristic structures fall on the cell width, the viscosity of liquid already has a significant effect. The mechanism of energy transfer from the small structures to the large ones is violated, and vortex formation does not occur.

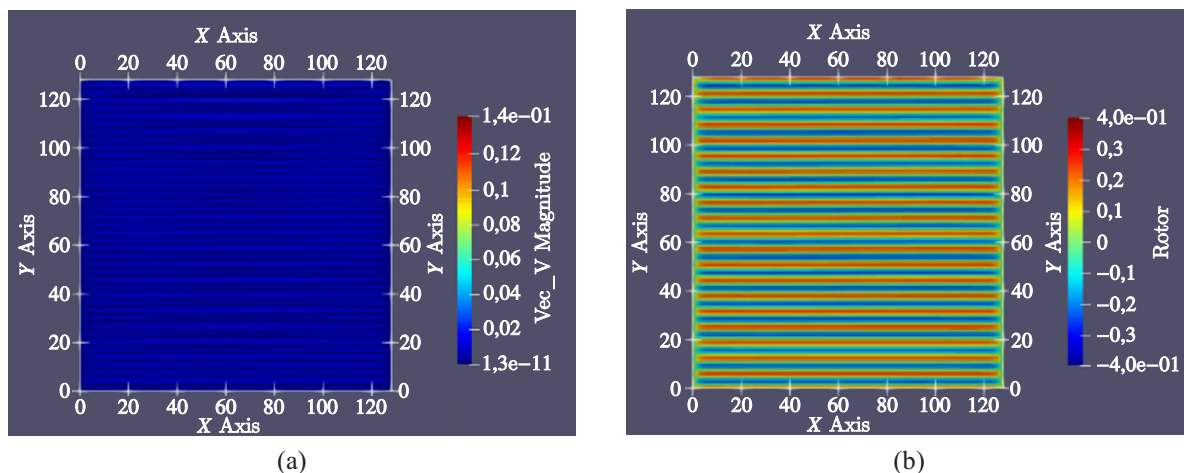


Figure 9. The velocity field (a) and the vorticity field (b) in the case of laminar fluid flow with the external force of high spatial frequency and $G = 0,05$ at the final stage of simulation

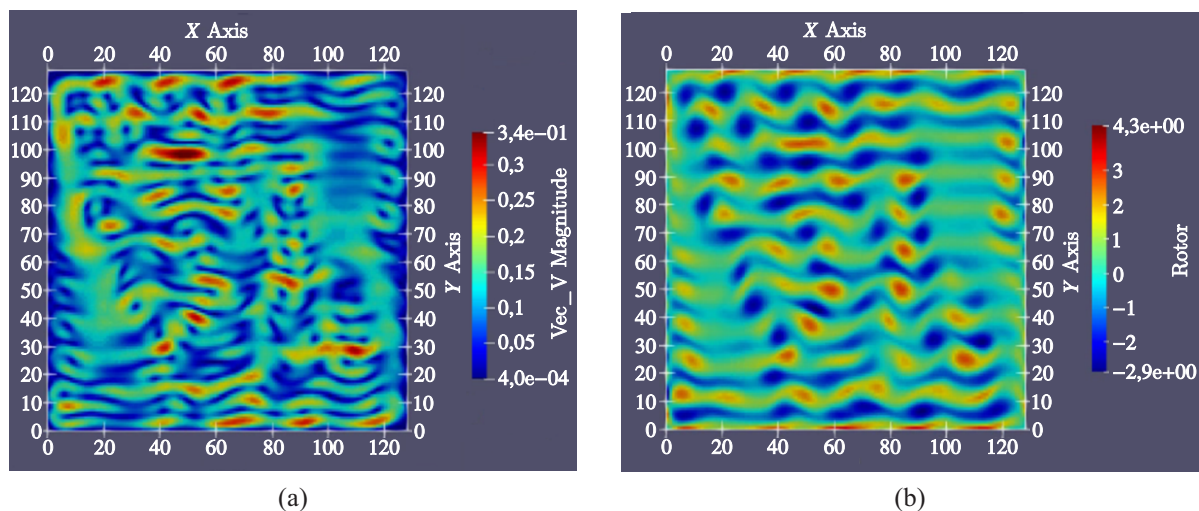


Figure 10. The velocity field (a) and the vorticity field (b) in the case of laminar fluid flow with the external force along the Ox axis equals $0,05 \sin(5y)$, $k_V = 10$ under the initial conditions (2) and (3), viscosity equals $\mu = 2 \text{ Pa} \cdot \text{s}$

If we increase the amplitude of the external force and make it equal to $G = 0,05 \text{ N/kg}$, while lowering its frequency to $k = 10$, then the streamlines repeating the lines in Figure 9, *a* begin to deform, bend, but the flow does not cease to be laminar (see Figure 10). Such initial conditions are, in a sense, the boundary between the laminar steady motion and turbulent. As noted above, viscosity is

the limiting factor that limits the flow of the kinetic energy along the inverse cascade and leads to its dissipation on smaller scales.

Let's consider equations (1) and the initial conditions (2) and (3) as, say, «standard» for the problem under consideration. In this formulation we use $G = 0,05$ N/kg, $\rho\beta = 0,5$ (s^2/m^2) is the artificial compressibility factor, $k = 5$ is the wave number for the external force, $k_V = 10$ is the wave number for the initial perturbation of the velocity components (the initial perturbation does not affect the final steady flow indeed).

When viscosity decreases, compressibility has to be reduced, because, firstly, the observed maximum velocities become comparable with the local speed of sound, and, secondly, the numerical scheme loses its stability. So when viscosity equals $\mu = 1$ Pa · s, the parameter of artificial compressibility $\rho\beta = 0,001$ (s^2/m^2), and the speed of sound becomes equal to $c \approx 31$ m/s. With steady motion, the formation of any stable vortex structures is not noticeable (Figure 11). The Reynolds number is $\text{Re} \approx 4712$.

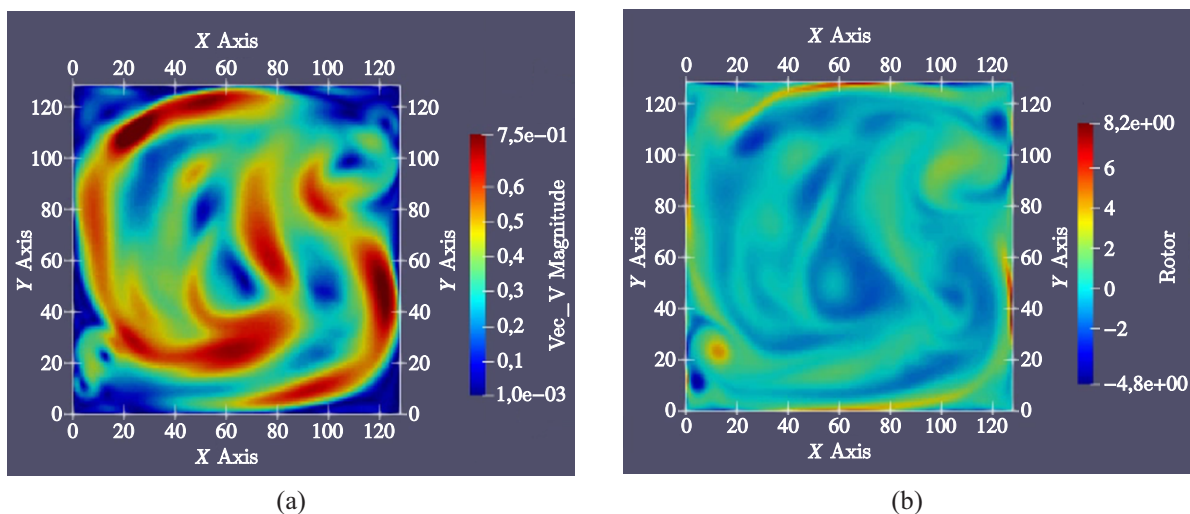


Figure 11. The velocity field (a) and the vorticity field (b) in the case of fluid flow with the external force along the Ox axis equals $0,05 \sin(5y)$, $k_V = 10$ under the initial conditions (2) and (3), viscosity equals $\mu = 1$ Pa · s

When viscosity equals $\mu = 0,1$ Pa · s, the compressibility factor remains equal to $\rho\beta = 0,001$ (s^2/m^2). In this case, the nucleating central vortex and a multitude of vortices rotating in the opposite direction at the cell periphery are observed at relatively large times (Figure 12). The Reynolds number in the last stages of calculation is $\text{Re} \approx 11938$.

In Figure 13 one can observe the vortex pattern formed upon a further decrease in viscosity to $\mu = 0,01$ Pa · s, and the compressibility factor to $0,0001$ (s^2/m^2). In this figure, one can see one centered vortex and the absence of small vortices located on the periphery of the cell, as it was seen in Figure 12. At the final stages of the calculation the Reynolds number is $\text{Re} \approx 8168$.

6. Conclusion

- 1) The vortex rotates with the frequency equal to the frequency of the vortex revolution around the center of the cell.
- 2) The steady quasistationary flow does not depend on the initial velocity distribution, but is determined by the parameters of the external influence.
- 3) An increase in the amplitude of the external force leads to an increase in the velocity of rotation of the vortex around the center of the cell.

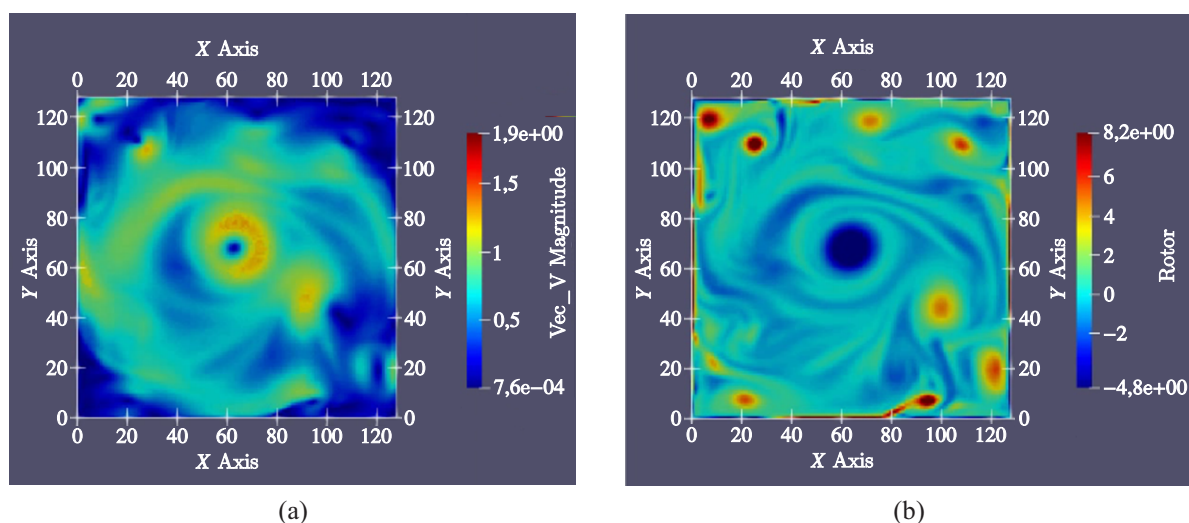


Figure 12. The velocity field (a) and the vorticity field (b) in the case of fluid flow with the external force along the Ox axis equals $0,05 \sin(5y)$, $k_V = 10$ under the initial conditions (2) and (3), viscosity equals $\mu = 0,1 \text{ Pa} \cdot \text{s}$

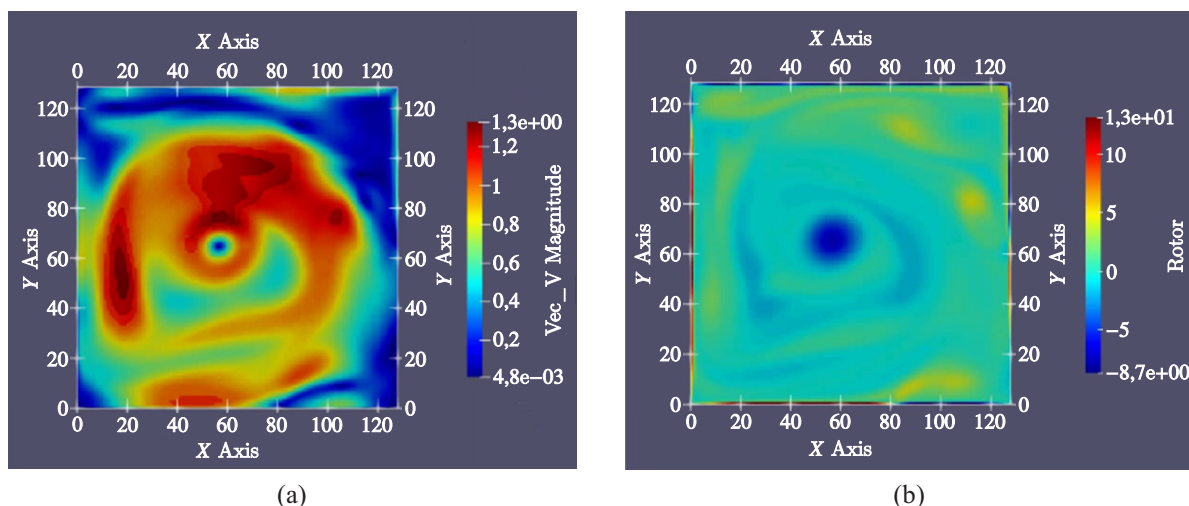


Figure 13. The velocity field (a) and the vorticity field (b) in the case of fluid flow with the external force along the Ox axis equals $0,05 \sin(5y)$, $k_V = 10$ under the initial conditions (2) and (3), viscosity equals $\mu = 0,01 \text{ Pa} \cdot \text{s}$

4) An increase in the spatial frequency of the external force leads to stabilization and laminarization of the flow. The mechanism of energy transfer through the inverse cascade of kinetic energy ceases due to its dissipation via the action of viscosity.

5) With an increased spatial frequency of the external force, a decrease in viscosity leads to the resumption of the mechanism of energy transfer along the inverse cascade due to a shift in the energy dissipation region to a region of smaller scales compared to the pump scale (frequency).

7. Acknowledgments

S. Fortova and V. Denisenko thank the support of the Russian Ministry of Science and Higher Education (State Assignment No. AAAA-A19-119041590048-0), A. Doludenko thanks the support of the Russian Ministry of Science and Higher Education (State Assignment No. 075-01056-22-00), I. Kolokolov thanks the support of the Russian Ministry of Science and Higher Education, V. Lebedev

thanks the support of the Russian Ministry of Science and Higher Education (grant No. 075-15-2019-1893).

References

- Anderson D. A., Tannehill J. C., Pletcher R. H.* Computational fluid mechanics and heat transfer. — Third Edition. — 2016.
- Batchelor G. K.* Computation of the Energy Spectrum in Homogeneous Two-Dimensional Turbulence // *Phys. Fluids*. — 1969. — Vol. 12, No. Suppl. II. — P. 233.
- Chertkov M. et al.* Dynamics of energy condensation in two-dimensional turbulence // *Phys. Rev. Lett.* — 2007. — Vol. 99. — P. 084501.
- Gledzer A. E. et al.* Structure functions of quasi-two-dimensional turbulence in a laboratory experiment // *J. Exp. Theor. Phys.* — 2011. — Vol. 113, No. 3. — P. 516–529.
- Gledzer E. B., Dolzhanskij F. V., Obukhov A. M.* Hydrodynamic type systems and their application. — Moscow: Nauka, 1981.
- Kolokolov I. V., Lebedev V. V.* Large-scale flow in two-dimensional turbulence at static pumping // *JETP Lett.* — 2017. — Vol. 106, No. 10. — P. 659–661.
- Kraichnan R. H.* Inertial Ranges in Two-Dimensional Turbulence // *Phys. Fluids*. — 1967. — Vol. 10. — P. 1417.
- Laurie J. et al.* Universal profile of the vortex condensate in two-dimensional turbulence // *Phys. Rev. Lett.* — 2014. — Vol. 113. — P. 254503.
- Sommeria J.* Experimental study of the two-dimensional inverse energy cascade in a square box // *J. Fluid Mech.* — 1986. — Vol. 170. — P. 139–168.
- Xia H., Shats M., Falkovich G.* Spectrally condensed turbulence in thin layers // *Phys. Fluids*. — 2009. — Vol. 21, No. 12. — P. 125101.